Langmuir

Article

A Simple, Fast and Sensitive assay for the detection of DNA, Thrombin and Adenosine triphosphate based on Dual-Hairpin DNA structure

Guangfeng Wang, Xiuping He, Gang Xu, Yanhong Zhu, Ling Chen, and Xiaojun Zhang

Langmuir, **Just Accepted Manuscript** • Publication Date (Web): 01 Oct 2013

A Simple, Fast and Sensitive assay for the detection of DNA, Thrombin and Adenosine triphosphate based on Dual-Hairpin DNA structure

Xiuping He, Guangfeng Wang*, Gang Xu, Yanhong Zhu, Ling Chen, Xiaojun Zhang*

Key Laboratory of Chem–Biosensing, Anhui province; Key Laboratory of Functional Molecular Solids, Anhui province; College of Chemistry and Materials Science, Anhui Normal University, Wuhu 241000, P R China

E-mail: xjzhang@mail.ahnu.edu.cn and wangyuz@mail.ahnu.edu.cn

Abstract

In the present study, based on multi-functional Dual-Hairpin DNA structure, a simple, fast and high sensitive assay for the detection of DNA, thrombin and Adenosine triphosphate (ATP) was demonstrated. DNA sequence labeled with Methylene blue (MB), which was designed as ss DNA matching with target DNA, thrombin or ATP aptamer, hybridized to the adjunct probe and formed the Dual-Hairpin structure on the electrode. With the hybridization of adjunct probe and the hairpin-like capture probe in the stem region, Dual-Hairpin was formed with outer and inner hairpins. By the conjugation of the target probe with the adjunct probe in the outer hairpin, the adjunct probe divorced from the Dual-Hairpin structure. The adjunct probe with signal molecules MB, attaching near or divorcing far from the

electrode produced electrochemical signal change, efficient electron transfer due to the fact that it was in proximity to the electrode. However, upon the hybridization with the perfect match target, the redox label with the target probe was forced away from the modified electrode thus resulting in the change of the Dual-Hairpin DNA conformation, which enables to impede the efficient electron transfer of MB, consequently, a detectable change of the electrochemical response. In addition, another highlight of this biosensor is its regenerability and stability owing to the merits of structure. And based on this Dual-Hairpin platform, the detection limit of DNA, thrombin and ATP were 50 nM, 3 pM and 30 nM, respectively. Moreover, this pattern also demonstrated excellent regenerability, reproducibility and stability. Additionally, given to its ease-of-use, simplicity in design, easy operations as well as regenerability and stability, the proposed approach may be applied as an excellent design prompter in the preparation for other molecular sensors.

Keyword: Dual-Hairpin; DNA; Thrombin; ATP; aptamer

1. Introduction

In the past decades, numerous biosensors have emerged to meet the increasing demands for point-of-care medical diagnostics and rapid methods for the specific detection of bioanalyte [1-7]. DNA sensors are of particular interest since DNA analysis plays a crucial role in a wide range of areas including diagnostics of genetic diseases, monitoring of infectious bacteria, analysis of forensic samples, and screening of

bioterrorism agents [8]. Meanwhile, the introduction of nucleic acid aptamers, with the merits of synthesis convenience, chemical stability, and flexibility in biosensor design, provides unprecedented opportunities to detect non-nucleic acid targets, which dramatically widens the application areas of nucleic acid sensors [9-12]. The development of optical or electrochemical nucleic-acid-based sensors for the analysis of DNA [13-16] and the detection of aptamer-substrate complexes [17-21] have attracted substantial interest. Nevertheless, electrochemical sensing comes to be one of the most promising approaches due to the rapid, reagentless, multiplexed and sensitive response, as well as low fabrication cost and operational convenience among various biosensing approaches available to date [22, 23].

Among the different electrochemical sensing platforms, it has been known for more than 50 years the most abundant structure of DNA in vivo is the double-stranded helical conformation, which is reported in 1953 by Watson and Crick for the first time [24], but other different DNA structures have been implemented by numerous studies, such as ss DNA [25], duplex sequences [26, 27], sandwich structure [28-30], super-sandwich structure [31-34], hand-in-hand structure [35], hairpin structure [36], dual-hairpin structure [37] and so on, which have received increasing attention because of the role they were proposed to play in transcription regulatory mechanisms [38]. Refer to hairpin DNA structure, although it can shorten the distance of the signal molecule and the surface of the electrode, which is effective to increase electrochemical response, it is hardly to take the determination of various substances to come true, owing to its poor flexibility [39-43]. However, in the Dual-Hairpin DNA structure, the adjunct probe with signal

molecule, can attach on the capture probe which functions as a fixer to immobilize the electrochemical signal molecules, thereby, minishing the distance between the signal molecules and the electrode surface and facilitating the electron transfer like the hairpin structure. Moreover, in the Dual-Hairpin DNA structure, the adjunct probe can be designed as some functional DNA sequences, such as G-rich, T-rich, or C-rich sequences, applying to detect the K^+, Hg^{2+} or Ag^+ ions, respectively. It is undoubted that the adjunct probe can also be devised as aptamers for any given target, ranging from small molecules to large proteins and even cells, thus making it possible to develop a wide range of aptamer-based biosensors due to the flexibility and designability of the adjunct probe. Briefly, the Dual-Hairpin DNA structure not only retaining the merits of hairpin DNA structure but also possessing the flexibility and variability of itself, can be used to detect DNA and other target molecules through the adjunct DNA sequence hybridizing with or divorcing from the capture DNA sequence. This Dual-Hairpin DNA structure based biosensor has significant advantages of simple fabrication process, high chemical stability and less interference with the detection environment.

Here we report on the development of multi-functional biosensing platforms that implement the functions of Dual-Hairpin DNA structure for simple and fast DNA sensing and aptasensing. Firstly, in the absence of the target (ie., ss DNA, thrombin or ATP), the stem-loop structure holds the redox label, methylene blue (MB) enabling efficient electron transfer due to the fact that it is in proximity to the electrode. However, upon the hybridization with the perfect match target, the redox label was

forced away from the modified electrode thus resulting in the change of the Dual-Hairpin DNA conformation, which enables to impede the efficient electron transfer of MB, consequently, a detectable change of the electrochemical response. In addition, another highlight of this biosensor is its regenerability and stability owing to the merits of structure. Most importantly, we believe that the use of this proposed biosensor is not limited to the three examples and is viable for the sensitive detection of other biomolecules, including RNA, proteins, and small molecules such as cocaine.

2. Experimental Section

2.1 Materials.

All HPLC-purified oligonucleotides were obtained from Sangon Biotechnology Co. Ltd (Shanghai, China). The sequence information of the probes and targets are as follows (Sequences of the used oligonucleotides S1: 5'-CTC TCA GTG ATT TTT TTA GTG AGA GAG-$(CH_2)_6$-SH-3' (the melting temperatures (Tm) of the designed duplexes was 68.1 ^oC, and 64.1 ^oC as the hairpin structure using Oligo Analyzer); S2 (the stem region completely matches with 10 bases of the stem region of S1, and the loop region is the aptamer of thrombin): 5'-MB-TCA CTT TGG TTG GTG TGG TTG GTC ACT-3'; S2a (one base mismatch with the stem region of S1): 5'-MB-TGA CTT TGG TTG GTG TGG TTG GTC ACT-3'; S2b (two bases mismatch with the stem region of S1): 5'-MB-TGA CTT TGG TTG GTG TGG TTG GTC AGT-3'; S2c (three bases mismatch with the stem region of S1): 5'-MB-TGA

GTT TGG TTG GTG TGG TTG GTG ACT-3'; S2d (four bases mismatch with the stem region of S1): 5'-MB-TGA GTT TGG TTG GTG TGG TTG GTG AGT-3'; S3(17 bases match with the loop region of S2): 5'-CCA ACC ACA CCA ACC AA-3'; S3a(two bases mismatch with the loop region of S2): 5'-CGA TCC ACA CCA ACC AA-3'; S3b (four bases mismatch with the loop region of S2): 5'-CGATCGAGACCAACCAA-3'; S3c(six bases mismatch with the loop region of S2): 5'-CGA TCG AGA GCT ACC AA-3'; S3d(eight bases mismatch with the loop region of S2): 5'-CGA TCG AGA GCT AGC TA-3'; S4(the loop region is the aptamer of ATP): 5'-MB-TCA CTA CCT GGG GGA GTA TTG CGG AGG AAG GTT CAC T-3'). The mismatches in the targets are underlined. Tris (hydroxymethyl) aminomethane (Tris), ATP and other reagents were also obtained from the Sinopharm Chemical Reagent Co. Ltd. (Shanghai, China). Ultrapure water (PSDK2-10-C) is used throughout all experiments.

2.2 Substrate DNA S1 self-assembled on gold electrode

Prior to the modification, the gold working electrode (2 mm diameter) was first polished sequentially with 0.3 and 0.05 μm alumina powder followed by ultrasonic cleaning with ethanol, and ultrapure water for 3 min each. Then the electrode was scanned in 0.1 M H_2SO_4 between −0.2 and 1.55 V at 100 mV/s 20 circles. After that, a steady-state redox wave was observed. Before use, oligonucleotides were dissolved in 0.05 M Tris-HCl buffer (pH 7.4) and stored at 4 ^{o}C for one night. The DNA solution was heated to 90 ^{o}C for 5 min to remove aggregates, and then cooled slowly to 30 ^{o}C [44-45]. The immobilization of the capture probe (S1) was performed by

dropping 30 μL of 10 mM Tris–HCl buffer containing 1.0 μM S1 probe on the cleaned gold electrode in a humidified chamber. The self-assembly through the thiol of S1 and Au atom was proceeded for 10 hours. Then the gold electrode was rinsed with water and incubated in 2 mM 6-mercaptohexanol in Tris-HCl (0.05 M, pH 7.4) (Tris-HCl buffer) for 2 hours to eliminate the nonspecific-bonded DNA. After being thoroughly rinsed with the washing buffer, the S1 probe modified gold electrode (S1/GE) was stored at 4 °C in HEPES buffer for further use.

2.3 Preparation of DNA sensor and aptasensor based on Dual-Hairpin DNA structure

The S1 probe modified electrodes were then incubated in the hybridization buffer, Tris-HCl buffer containing 3 μM S2 probe, at 37 °C for 5 h to form the Dual-Hairpin DNA structure modified electrode (S2/S1/GE). In the control experiments, S2a, S2b, S2c or S2d which has one, two, three and four mismatches with S1, respectively replaced S2 to study the selectivity. Under the same conditions, S4 substituting S2 was prepared to form ATP aptasensors (S4/S1/GE).

2.4 Detection of DNA, aptasensors with Dual-Hairpin DNA structure

For the detection of DNA sequence S3 or thrombin, the S2 modified electrodes were then incubated in the hybridization Tris-HCl buffer (pH 7.4) containing S3 or thrombin with different concentrations, and formed the modified electrode S3+ S2/S1/GE or thrombin+S2/S1/GE, respectively. When finishing incubation, the modified electrodes were thoroughly rinsed, dried with N2 before electrochemical measurements. Under the same conditions, S4 substituting S2 for preparing S4/S1/GE

was incubated with different concentrations of ATP named S2/S1/GE (ATP+S4/S1/GE) as ATP biosensor.

2.5 Instrumentation and Procedure.

All the electrochemical experiments were carried out at room temperature. Electrochemical measurements were conducted on CHI 660 electrochemical analyzers (CH Instruments). Cyclic voltammetry (CV) was performed in Tris-HCl buffer within the potential range from −0.4 to 0 V using scan rate of 100 mV/s. Electrochemical impedance spectra (EIS) was performed in PBS (0.05 M, pH 7.4) containing 5 mM $Fe(CN)_6^{3-}/Fe(CN)_6^{4-}$ and 0.1 M KCl in the frequency range from 0.1 Hz to 100 kHz with 5 mV as the amplitude at a polarization potential of -0.18 V. All the electrochemical experiments were carried out at room temperature.

3. Results and discussion

3.1 Strategy of the assay

Scheme 1 illustrated the fabrication of the simple DNA sensors based on Dual-Hairpin DNA structure. First, the S1 could be stabilized by a combination of Au-S bonding on the gold electrode and formed a hairpin DNA structure due to the designed five pairs of bases match in the stem region. The target DNA S2 modified with MB, another five pairs of bases of this sequence matching with S1 in the other part of the stem region, was captured by the immobilized S1 forming Dual-Hairpin DNA structure S2/S1/GE. This Dual-Hairpin DNA model was easily formed, current of MB presented. With the addition of S3, containing 17 bases completely complementary with the loop part of S2, it would enable S2 to divorce from the S1

modified electrode. Because the S2 which contained the signal molecules MB was now far away from the electrode, thus the current would drop sharply. With the increasing concentration of S3, the resulting current would decline gradually. On the basis of the drop electrochemical signal, this DNA sensor could be used to detect DNA sequence, S3. However, if S2 was designed as the aptamer, the proposed can be aptasensors, such as thrombin and ATP aptasensors, as shown in Part II and III respectively, in Scheme 1.

3.2 CV and EIS of the modification procedure

As we know, CV is an effective tool to characterize the interface properties of different film modified electrodes. To examine the electroanalytical performance of the modified electrodes, CV was employed first in the Tris-HCl buffer. As shown in Fig. 1A, when GE was modified with S1 (curve b), a small CV response was observed, compared with that of the bare GE (curve a). Then, with S2 further modified onto S1/GE, on the S2/S1/GE there existed an obvious electrochemical response (curve c). Because MB was labelled at the 5' end of S2, the electrochemical response could be explained by the reduction of MB at about -0.25 V implying that S2 was successfully assembled on GE as designed. EIS is another technique for characterizing the properties of surface-modified electrodes. In the Nyquist plot of EIS, the semicircle part at higher frequencies corresponds to the electron transfer limited process, and the linear part at lower frequencies corresponds to the diffusion process. The electron-transfer resistance (*R*et) was described using the semicircle diameter of EIS. To prove our design, we also conducted electrochemical impedance measurements to study the

interface properties of different modified electrode. As shown in Fig. 1B (curve a), the impedance spectrum of the bare GE included almost no semicircle domain. When the electrode was modified with S1, the semicircle was larger due to the formation of a negatively charged interface, which may electrostatically repel the also negatively charged redox species $[Fe(CN)_6]^{3-/4-}$ (curve b). After the electrode was further hybridized with S2, the diameter of the semicircle continued to increase (curve c), indicating the further loading of negatively charged DNA strands. All these impedance spectra were coherent as predicted, too. In a control experiment (Fig. 1C), if S1/GE hybridized with S2a, S2b, S2c and S2d respectively, the CV response was much smaller compared with curve c. Because S2a, S2b, S2c and S2d had one, two, three and four mismatches with S1, respectively, with the match degree decreasing from S2a to S2d with S1, the EIS decreased which again proved our design.

3.3. Optimization of external conditions

Experimental conditions were optimized in order to achieve high sensitivity, and the optimization of the variables of the system was shown in Fig. 2. Fig. 2 depicted the effect of pH, temperatures and time-dependent voltammetric waves to form the Dual-Hairpin DNA structure. As the time of interaction was prolonged, the currents increased as shown in Fig. 2A. Upon incubation time was more than 5 hours, the signal of current showed a level indicating that the reaction may complete in 5 hours. Therefore, 5 h was chosen as optimization of incubation time used in the experiments. Furthermore, Fig. 2B and C outlined the electrocatalytic currents on S2/S1/GE,

resulting that hybridization temperatures at 35 °C under pH 7.4 was the best. In order to optimize the amount of Dual-Hairpin DNA structure units modified on the gold electrode, we have carried out a series experiments with different concentrations of S2. Consequently, when the concentration of S2 was 3 μM, the CV responses reached a level suggesting maybe the density of the Dual-Hairpin DNA structure on the gold electrode was saturated. Ultimately, we chose hybridization time 5 h, incubation temperature 35 °C, pH 7.4 and the 3 μM S2 as the optional experimental conditions.

3.4 Detection of S3 and the selectivity of the sensor

Under the optimal conditions, we anticipated a quantitative nature for S3 on the basis of Dual-Hairpin DNA structure. Fig. 3A gave CV responses of S2/S1/GE (curve a) and S3+S2/S1/GE (curve b). As shown in Fig. 3A, the current signal of curve b inclined obviously, implying that ss DNA S3 was able to force the S2 away from the electrode due to the bases pairing. At the same time, the EIS fell after S2/S1/GE incubated with S3. The proposed DNA sensor effective to detect S3 was proved by these consequences. Fig. 3C gave DPV responses of S3 with varying concentrations on the Dual-Hairpin DNA structure S2/S1/GE. We observed dynamically decreased DPV peaks current in response to S3 of increasing concentrations within the range from 0.15 to 0.9 μM with an achieved detection limit of 50 nM. The resulting calibration curve was depicted in Fig. 3D. A further aspect to consider related to the specificity of the sensing platform and the possibility to discriminate bases mismatches. As exhibited in Fig. 3E, we also challenged the sensor with four different

mismatched targets (i.e., S3a, S3b, S3c and S3d). Both 2 and 4 bp mismatch targets (S3a and S3b) have similar responses like S3, due to the fact that these two mismatch bases took lower percents of the whole 17 bases. It was worth mentioning that other mismatched sequences exhibited significant difference from that of S3 on the electrochemical intensity. revealing good selectivity of the proposed approach.

3.5 Regenerability, reproducibility and stability of the sensor

Additionally, the sensor's regenerability was another feature of this class of DNA sensors. In order to test the sensor's regenerability, we simply rinsed the hybridized sensor for 30 sec using room temperature water. The data of its regenerability was shown in Fig. 1D inset. We defined initial CV currents of MB were 100%, when the S3 was modified on the S2/S1/GE, the response was decreased to 13%. However, with the addition of S2, S2/S1/GE was fabricated again, and the CV currents of MB increased to 84%. This process was defined as the sensor's regenerability. Although minor loss in MB currents was observed, it also posted this sensor's regeneration. Moreover, a total number of six group DNA biosensors had been tested for the proposed sensor's reproducibility. Each group was prepared in the same condition. The R.S.D. % of the response to the S3 of six different biosensors belonging to the same concentration was less than 6%. At the same time, CV curves of S2/S1/GE for 10 cycles were shown in Fig. 1D, and it was worth noting that the signal of MB reduced little indicating the reproducibility of the sensor was satisfactory. These results are averages from 3 different sensors, highlighting the sensor's reusability and reproducibility. Given the high sensitivity and selectivity of this electrochemical DNA

sensor, we also tested its stability. After the biosensors were stored in refrigerator for a period of one week, 91.7 % of the initial current response for DNA (0.90 μM as an example) could be remained implying that the proposed method possess an acceptable stability.

3.6 Thrombin sensor based on Dual-Hairpin DNA Structure

The use of Dual-Hairpin DNA structure as template for biosensing was further extended to develop aptasensors using thrombin and ATP as the examples. Scheme 1 Part II depicted the configuration of thrombin sensor based on Dual-Hairpin structure. S1 was immobilized on GE surface, contains five bases matching in the stem region which was the same with that of the above DNA sensor. When the incubation solution involved S2, S2 would conjugate with S1. In the presence of thrombin, by the conjugation of thrombin and its aptamer, S2, S2 with electrochemical signal molecules MB broke away from the electrode and the electrochemical signal decreased. As shown in Fig. 4A, the CV response of S2/S1/GE incubated with thrombin is much smaller than that of S2/S1/GE. At the same time, the Ret of thrombin+S2/S1/GE was smaller (Fig. 4B, curve b) compared with that of S2/S1/GE (curve a) indicating that the addition of thrombin enabled the S2 to deprive from the modified electrode. Given to Fig. 4A and B, this sensor could be used to detect thrombin attributing to its effect on the electrochemical signal. Fig. 4C and D showed the DPV responses and corresponding calibration curve of current vs. increasing concentrations of thrombin within the range from 10^{-11} to 10^{-2} M with an

achieved detection limit of 3 pM. Fig. 4E showed the selectivity of the sensor was tested by substituting thrombin. The modified electrodes exhibited a remarkable peak current drop for thrombin, and hardly responded to other proteins, indicating that the sensor had an impressive specificity toward the detection of thrombin. In order to testify the selectivity of the Dual-Hairpin DNA structure assay, we chose S2/S1/GE for thrombin analysis in Tris-HCl buffer containing 10^{-9} M thrombin and other equal concentration proteins for example. As shown in Fig. 4F, when the incubation solution contained thrombin and the other three proteins on the S2/S1/GE, the CV responses declined obviously. However, if there were no thrombin, the signal almost kept unchanged, implying that the proposed sensor could be applied into complex sample. Such excellent selectivity should be ascribed to the merits of aptamer-thrombin to the signal probe. This platform clearly showed that this Dual-Haipin structure provided a formwork for DNA based sensor.

3.7 ATP sensor on the base of Dual-Hairpin DNA Structure

Finally, the Dual-Hairpin sensing platform was applied to detect ATP (Scheme 1 Part III). After S4 was immobilized on S1/GE surface, ATP conjugated with S4 due to that the designed S4 was the aptamer of ATP which made S4 separate from the S1/GE. Because S4 also had a signal molecule MB at 5' end just like S2, the hybridization and separation of S4 from the surface of the electrode would alter the electrochemical signal, which then provided a possibility for the analysis of ATP. Fig. 5A and B showed the CV and EIS character of the proposed ATP sensor. And as we see, with the addition of ATP, the value of current and Ret decreased, which may be due to the

fact that the combination of ATP and the S4 forcing the S4 away from the electrode. Thus, we suggested the proposed aptasensor may be effective to detect ATP. We then studied the DPV response of the proposed sensor with different concentrations of ATP. The DPV response changed at different concentrations of ATP depicted in Fig. 5C with the concentration from 10^{-7} to 1 M. The resulting calibration curve was shown in Fig. 5D. Evidently, the analyte ATP could be detected at 10^{-7} M with the limit detection of 30 nM. In addition, the control experiments also revealed no obviously changes upon guanosine triphosphate (GTP), uridine triphosphate (UTP), cytidine triphosphate (CTP) (equal concentration) implying that the proposed sensor was selective for ATP due to the specific binding of ATP.

4. Conclusions

The present study introduced a Dual-Hairpin DNA structure as a versatile scaffold for different sensors. Specifically, we developed DNA and aptamers sensing platforms. Upon the detection of the respective analytes, the Dual-Hairpin structure was changed and the signal decreased. The low detection limits, wide linear range and operational stability for the analysis of DNA, thrombin and ATP were satisfactory. In summary, when compared to the previously DNA sensor, this sensor was equally rapid, specific and selective, but with added features of regenerability owing to its architecture. The highlight of this work is to produce a simple, fast and high assay platform for the determination of DNA, thrombin and ATP. Additionally, the DNA displacement mechanism used here could potentially be adapted to the design of other electrochemical DNA or aptamer-based sensors.

Acknowledgment

This work was financially supported by the projects (21073001, 21005001 and 21371007) from National Natural Science Foundation of China, Anhui Provincial Natural Science Foundation (1208085QB28), Natural Science Foundation of Anhui (KJ2012A139) and the Program for Innovative Research Team at Anhui Normal University.

Reference

(1) Kissenger, P. T. Biosensors-a perspective. *Biosens. Bioelectron.* **2005**, *20*, 2512-2516.

(2) Gooding, J. J. Biosensor technology for detecting biological warfare agents: recent progress and future trends. *Anal. Chimica. Acta*. **2006**, *559*, 137-151.

(3) Wang, J.; Musameh, M.; Lin, Y. Solubilization of carbon nanotubes by nation toward the preparation of amperometric biosensors. *J. Am. Chem. Soc.*, **2003**, *125*, 2408-2409.

(4) Wang, J. From DNA biosensors to gene chips. *Nucl. Acids Res.* **2000**, *28*, 3011-3016.

(5) Besteman, K.; Lee, J.; Wiertz, F. G. M.; Heering, H. A.; Dekker, C. Enzyme-coated carbon nanotubes as single-molecule biosensors. *Nano Letters*, **2003**, *3*, 727-730.

(6) Chen, R. J.; Bangsaruntip, S.; Drouvalakis, K. A.; Kam, N. W. S.; Shim, M.; Li, Y.; Kim, W.; Utz, P. J.; Dai, H. J. Noncovalent functionalization of carbon nanotubes for highly specific electronic biosensors. *PNAS* **2003**, *29*, 4984-4989.

(7) Katz, E.; Willner, I. Probing biomolecular interactions at conductive and semiconductive surfaces by impedance spectroscopy: Routes to impedimetric immunosensors, DNA-sensors, and enzyme biosensors. *Electroanalysis* **2003**, *15*, 913-947.

(8) Debouck, C.; Goodfellow, P. N. DNA microarrays in drug discovery and development. *Nat. Genet.* **1999**, *21*, 48-50.

(9) Joyce, G. F. Directed evolution of nucleic acid enzymes. *Annu. Rev. Biochem.* **2004**, *73*, 791-836.

(10) Song, S.; Wang, L.; Li, J.; Zhao, J.; Fan, C. Aptamer-based biosensors. *Trends Anal. Chem*. **2008**, *27*, 108-117.

(11) Liu, J. W. ; Cao, Z. H. ; Lu, Y. Functional nucleic acid sensors. *Chem. Rev.* **2009**, *109*, 1948-1998.

(12) Osborne, S. E.; Ellington, A. D. Nucleic Acid Selection and the Challenge of Combinatorial Chemistry. *Chem. Rev.* **1997**, *97*, 349-370.

(13) Gooding, J. J. Electrochemical DNA Hybridization Biosensors. *Electroanalysis* **2002**, *14*, 1149-1156.

(14) Drummond, T. G.; Hill, M. G.; Barton, J. K. Electrochemical DNA sensors. *Nat. Biotechnol*. **2003**, *21*, 1192-1199.

(15) Patolsky, F.; Weizmann, Y.; Willner, I. Redox-active nucleic-acid replica for the amplified bioelectrocatalytic detection of viral DNA. *J. Am. Chem. Soc*. **2002**, *124*, 770-772.

(16) Wang, F.; Elbaz, J.; Teller, C.; Willner, I. Amplified detection of DNA through an autocatalytic and catabolic DNAzyme-mediated process. *Angew. Chem. Int. Ed*. **2011**, *50*, 295-299.

(17) Willner, I.; Zayats, M. Elektronische Aptasensoren *Angew. Chem. Int. Ed.* **2007**, *119*, 6528-6538.

(18) Willner, I.; Zayats, M. Electronic aptamer-based sensors. *Angew. Chem. Int. Ed.* **2007**, *46*, 6408-6418.

(19) Wang, G.; Wang, Y.; Chen, L.; Choo, J. Nanomaterial-assisted aptamers for optical sensing. *Biosens. Bioelectron.* **2010**, *25*, 1859-1868.

(20) Balamurugan, S.; Obubuafo, A.; Soper, S. A.; Spivak, D. A. Surface immobilization methods for aptamer diagnostic applications. *Anal. Bioanal. Chem*. **2008**, *390*, 1009-1021.

(21) Lee, J. O.; So, H.-M.; Jeon, E. K.; Chang, H.; Won, K.; Kim, Y. H. Aptamers as molecular recognition elements for electrical nanobiosensors. *Anal. Bioanal. Chem.* **2008**, *390*, 1023-1032.

(22) Grieshaber, D.; MacKenzie, R.; Vörös, J.; Reimhult, E. Electrochemical biosensors-Sensor principles and architectures. *Sensors*, **2008**, *8*, 1400-1458.

(23) Palec □ek, E.; Bartos □ík, M. Electrochemistry of nucleic acids. *Chem. Rev.* **2012**, *112*, 3427-3481.

(24) Watson, J. D.; Crick, F. H. C. A Structure for Deoxyribose Nucleic Acid *Nature* **1953**, *171*, 737-738.

(25) Wu, Z.; Zhen, Z.; Jiang, J. H.; Shen, G. L.; Yu, R. Q. Fluorescent sensors based on aptamer self-assembly. *J. Am. Chem. Soc.* **2009**, *131*, 12325-12332.

(26) Cao, Y.; Zhu, S.; Yu, J.; Zhu, X.; Yin, Y.; Li, G. X. Protein detection based on small molecule-linked DNA. *Anal. Chem.* **2012**, *84*, 4314-4320.

(27) Liu, Y. H.; Li, H. N.; Chen, W.; Liu, A. L.; Lin, X. H.; Chen, Y. Z. Bovine serum albumin-based probe carrier platform for electrochemical DNA biosensing. *Anal. Chem*. **2013**, *85*, 273-277.

(28) Ikebukuro, K.; Kiyohara, C.; Sode, K. Novel electrochemical sensor system for protein using the aptamers in sandwich manner. *Biosens. Bioelectron.* **2005**, *20*, 2168-2172.

(29) Ikebukuro, K.; Kiyohara, C.; Sode, K. Electrochemical detection of protein using a double aptamer sandwich. *Anal. Lett.* **2004**, *37*, 2901-2909.

(30) Polsky, R.; Gill, R.; Kaganovsky, L.; Willner, I. Nucleic acid-functionalized Pt nanoparticles: Catalytic labels for the amplified electrochemical detection of biomolecules. *Anal. Chem.* **2006**, *78*, 2268-2271.

(31) Tang, J.; Hou, L.; Tang, D. P.; Zhang, B.; Zhou, J.; Chen, G. N. Hemin/G-quadruplex-based DNAzyme concatamers as electrocatalysts and biolabels for amplified electrochemical immunosensing of IgG1. *Chem. Commun*. **2012**, *48*, 8180-8182.

(32) Jiang, Y.; Liu, N.; Guo, W.; Xia, F.; Jiang, L. Highly-efficient gating of solid-state nanochannels by DNA supersandwich structure containing ATP aptamers: a nanofluidic IMPLICATION logic device. *J. Am. Chem. Soc.* **2012**, *134*, 15395-15401.

(33) Wang, G. F.; He, X. P.; Chen, L.; Zhu, Y. H.; Zhang, X. J.; Wang, L. Conformational Switch for Cisplatin with Hemin/G-Quadruplex DNAzyme Supersandwich Structure. *Biosens. Bioelectron*. **2013**, *50*, 210-216.

(34) Wang, G. F.; He, X. P.; Wang, L.; Zhang, X. J. A Folate Receptor Electrochemical Sensor Based on Terminal Protection and Supersandwich DNAzyme Amplification. *Biosens. Bioelectron.* **2013**, *42*, 337-341.

(35) Li, C.; Wang, Z.; Gao, T.; Duan, A.; Li, G. Fabrication of hand-in-hand nanostructure for one-step protein detection. *Chem. Commun*. **2013**, *49*, 3760-3762.

(36) Wei, X.; Lin, W.; Ma, N.; Luo, F.; Lin, Z.; Guo, L.; Qiu, B.; Chen, G. Sensitive fluorescence biosensor for folate receptor based on terminal protection of small-molecule-linked DNA. *Chem. Commun.* **2012**, *48*, 6184-6186.

(37) Wu, H.; Liu, S.; Jiang, J.; Shen, G.; Yu, R. A sensitive electrochemical biosensor for detection of DNA methyltransferase activity by combining DNA methylation-sensitive cleavage and terminal transferase-mediated extension. *Chem. Commun.* **2012**, *48*, 6280-6282.

(38) Wang, G. F.; Huang, H.; Wang, B. J.; Zhang, X. J.; Wang, L. A supersandwich multienzyme-DNA label based electrochemical immunosensor. *Chem. Commun.* **2012**, *48*, 720-722.

(39) Wadkins, R. M. Targeting DNA secondary structures. *Curr. Med. Chem.* **2000**, *7*, 1-15.

(40)Vallée-Be´lisle, A.; Ricci, F.; Uzawa, T.; Xia, F.; Plaxco, K. W. Bioelectrochemical switches for the quantitative detection of antibodies directly in whole blood. *J. Am. Chem. Soc.* **2012**, *134*, 15197-15200.

(41) Farjami, E.; Clima, L.; Gothelf, K.; Ferapontova, E. E. "Off-on" electrochemical hairpin-DNA-based genosensor for cancer diagnostics. *Anal. Chem.* **2011**, *83*, 1594-1602.

(42) Yu, Z.; Lai, R. Y. Effect of signaling probe conformation on sensor performance of a displacement-based electrochemical DNA sensor. *Anal. Chem.* **2013**, *85*, 3340-3346.

(43) Kang, D.; Zuo, X.; Yang, R.; Xia, F.; Plaxco, K. W.; White, R. J. Comparing the properties of electrochemical-based DNA sensors employing different redox tags. *Anal. Chem.* **2009**, *81*, 9109-9113.

(44) Wang, L. H.; Wen, Y.; Liu, J.; Zhou, J.; Li, C.; Wei, C. Y. Promoting the formation and stabilization of human telomeric G-quadruplex DNA, inhibition of telomerase and cytotoxicity by phenanthroline derivatives. *Org. Biomol. Chem.* **2011**, *9*, 2648-2653.

(45) Schaffitzel, C.; Postbereq, J.; Paeschke, K.; Lipps, H. J.; Probing Telomeric G-Quadruplex DNA Structures in Cells with In Vitro Generated Single-Chain Antibody Fragments. *G-Quadruplex DNA Methods in Molecular Biology*, **2010**, *608*, 159-181.

Captions:

Scheme 1. Fabrication process of the electrochemical determination of DNA, Thrombin and ATP based on Dual-Hairpin DNA structure

Fig. 1 (A) CV of different conditions in Tris-HCl buffer: bare GE (a); S1/GE (b); S2/S1/GE (c). (B) Nyquist plot for EIS measurements for different modified electrodes: bare GE (a), S1/GE (b), S2/S1/GE (c). (C) Selectivity of Dual-Hairpin DNA Structure for S2 assay (3 μM S2 or equal concentration of other sequences as example). (D) CV responses of S2/S1/GE for 10 cycles and Sensor interrogation-regeneration plot (inset).

Fig. 2 Optimization of experimental conditions including pH value (A), incubation temperature (B), hybridization time (C) and the concentration of S2 (D).

Fig. 3 (A) CV and (B) EIS on Dual-Hairpin DNA structure S2/S1/GE (a); S3+S2/S1/GE (b), 0.3 μM S3 as example; (C) DPV and corresponding calibration curve of current vs. the concentration of S3: (a–g) 0; 0.15; 0.2; 0.3; 0.4 ;0.5; 0.9 μM in Tris-HCl buffer; and (E) Selectivity of S3 analysis in Tris-HCl buffer (0.9 μM S3 or equal concentration of other sequences as example).

Fig. 4 (A) CV on S2/S1/GE (a), Thrombin+S2/S1/GE (b); (B) EIS: S2/S1/GE (a); Thrombin+S2/S1/GE (b), 10^{-8} M Thrombin as example; (C) DPV in the presence of various concentrations of Thrombin: (a–h) 0; 10^{-11}; 10^{-10}; 10^{-9}; 10^{-8} ; 10^{-7}; 10^{-6}; 10^{-2} M in Tris-HCl buffer; (D) The corresponding calibration curve of current vs. the concentration of thrombin; (E) Selectivity of the Dual-Hairpin DNA structure assay for thrombin analysis in Tris-HCl buffer (0.01 M thrombin or other equal concentration proteins as example); (F) Selectivity of the Dual-Hairpin DNA structure assay for thrombin analysis in Tris-HCl buffer containing 10^{-9} M thrombin and other equal concentration proteins or only containing other three equal concentration proteins as example.

Fig. 5 (A) CV and (B) EIS on Dual-Hairpin DNA structure S4/S1/GE (a); ATP+S4/S1/GE (b), 10^{-4} M ATP as example; (C) DPV and corresponding calibration curve of current vs. the concentration of ATP: (a–h) 0; 10^{-7}; 10^{-6}; 10^{-5}; 10^{-4}; 10^{-3}; 10^{-2}; 1 M in Tris-HCl buffer; and (E) Selectivity of ATP analysis in Tris-HCl buffer (1 M thrombin or other equal concentration substances as example).

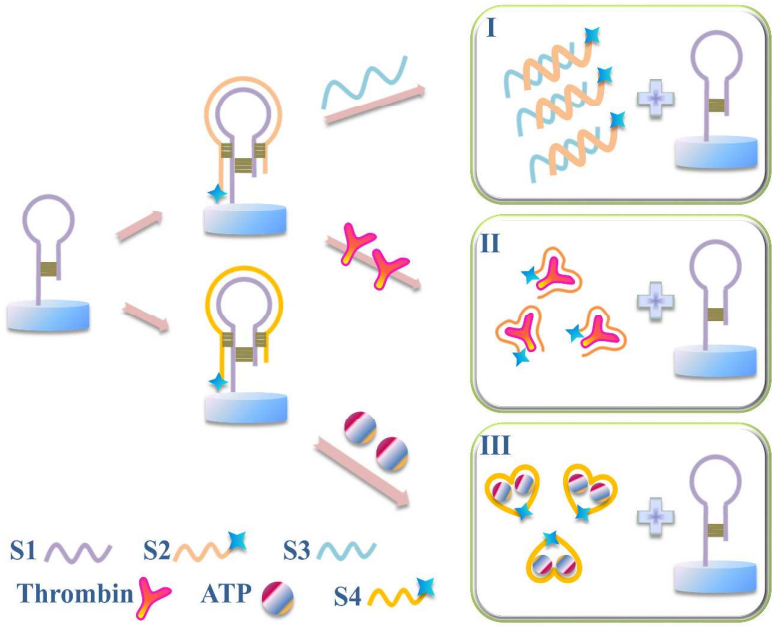

Scheme 1. Fabrication process of the electrochemical determination of DNA, Thrombin and ATP based on Dual-Hairpin DNA structure

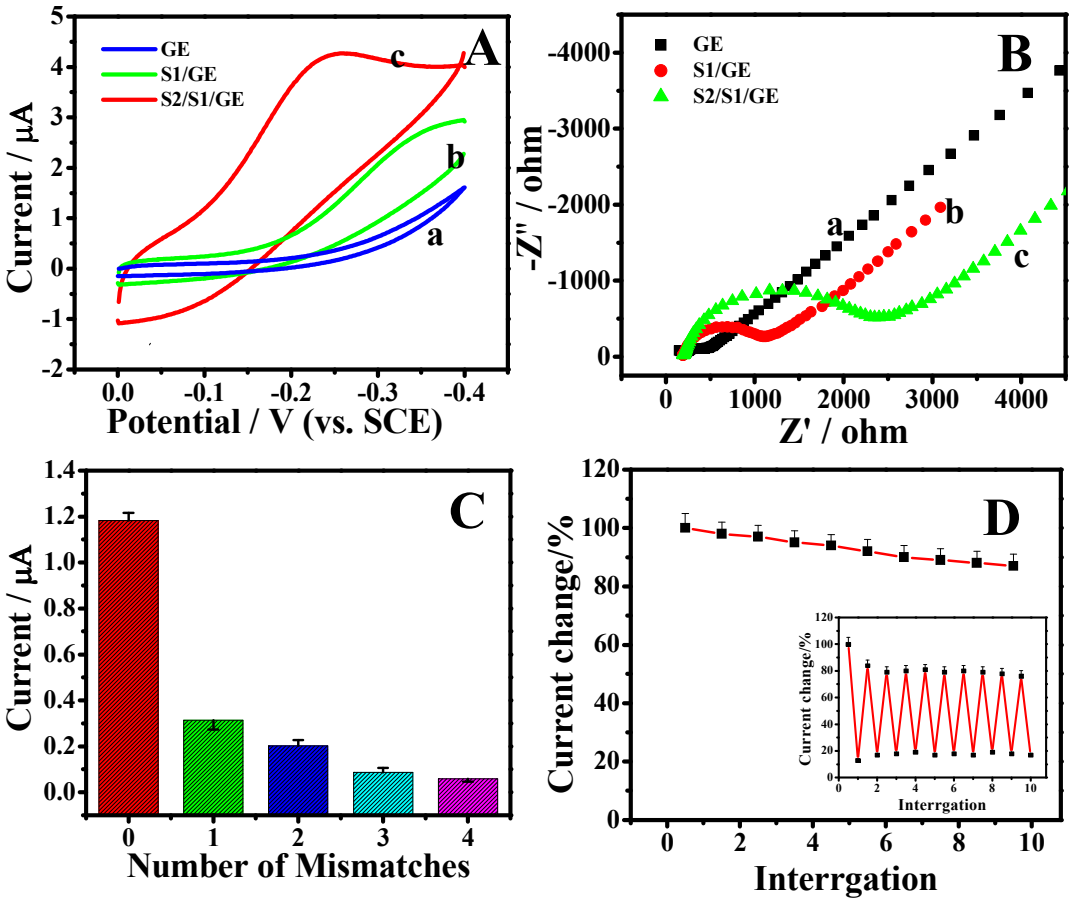

Fig. 1 (A) CV of different conditions in Tris-HCl buffer: bare GE (a); S1/GE (b); S2/S1/GE (c). (B) Nyquist plot for EIS measurements for different modified electrodes: bare GE (a), S1/GE (b), S2/S1/GE (c). (C) Selectivity of Dual-Hairpin DNA Structure for S2 assay (3 μM S2 or equal concentration of other sequences as example). (D) CV responses of S2/S1/GE for 10 cycles and Sensor interrogation-regeneration plot (inset).

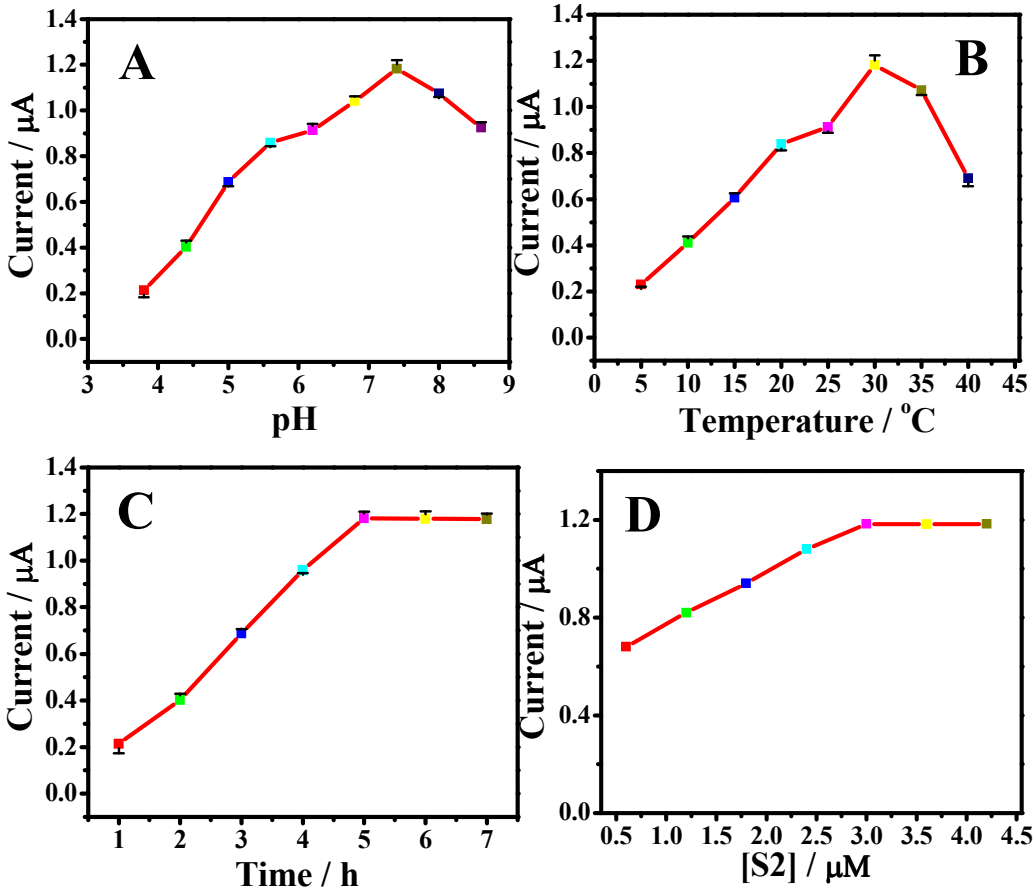

Fig. 2 Optimization of experimental conditions including pH value (A), incubation temperature (B), hybridization time (C), and the concentration of S2 (D).

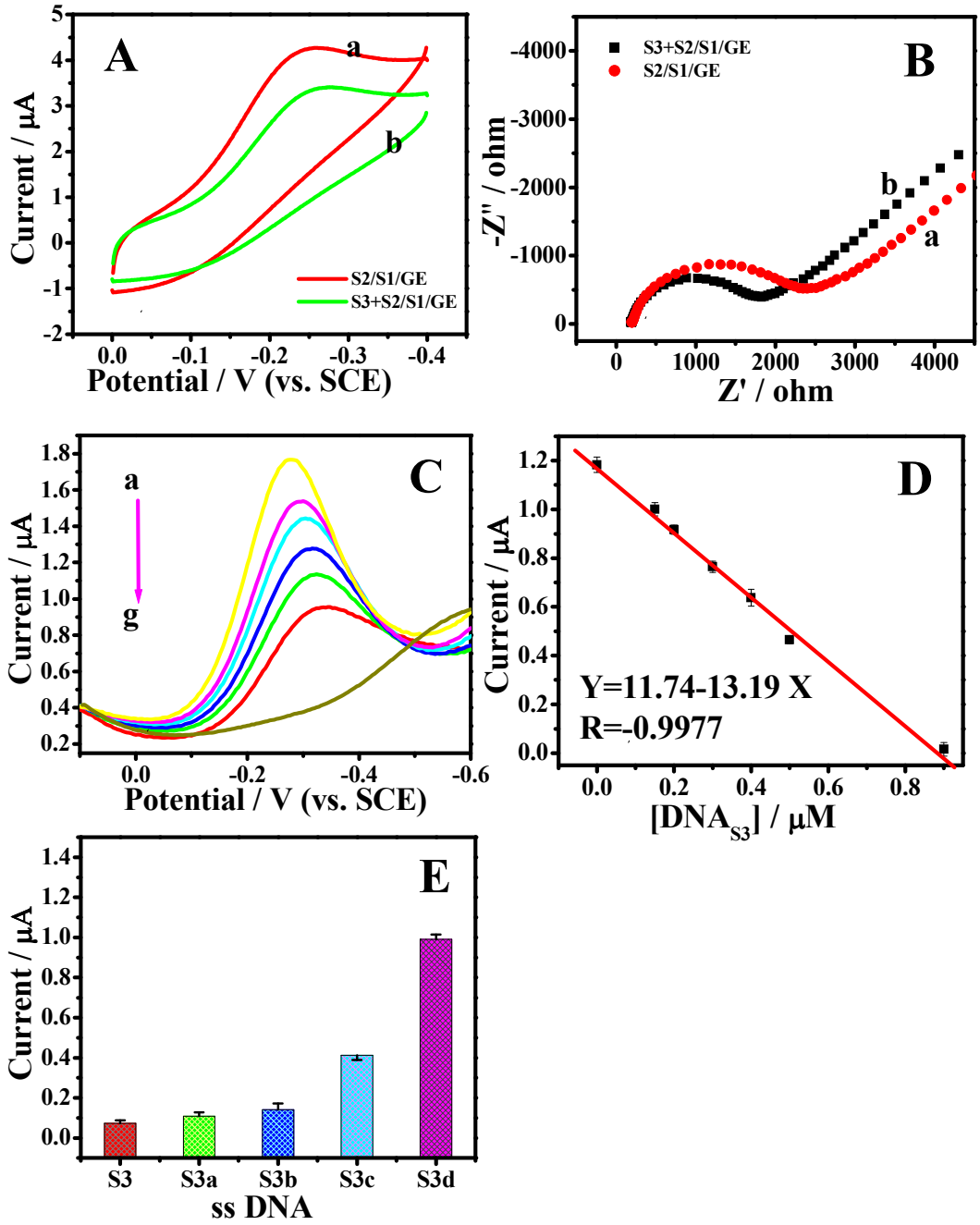

Fig. 3 (A) CV and (B) EIS on Dual-Hairpin DNA structure S2/S1/GE (a); S3+S2/S1/GE (b), 0.3 μM S3 as example; (C) DPV and corresponding calibration curve of current vs. the concentration of S3: (a–g) 0; 0.15; 0.2; 0.3; 0.4 ;0.5; 0.9 μM in Tris-HCl buffer; and (E) Selectivity of S3 analysis in Tris-HCl buffer (0.9 μM S3 or equal concentration of other sequences as example).

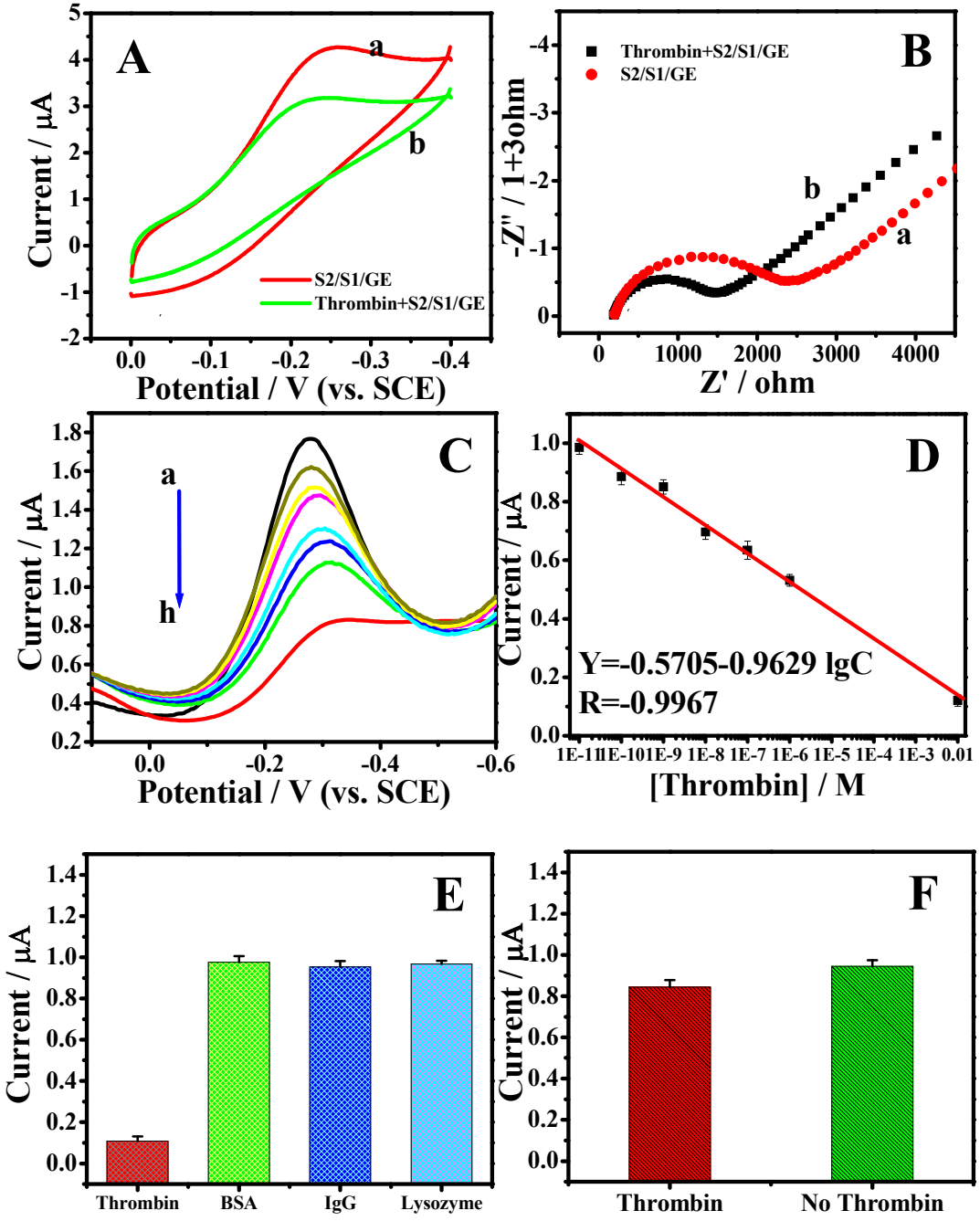

Fig. 4 (A) CV on S2/S1/GE (a), Thrombin+S2/S1/GE (b); (B) EIS: S2/S1/GE (a); Thrombin+S2/S1/GE (b), 10^{-8} M Thrombin as example; (C) DPV in the presence of various concentrations of Thrombin: (a–h) 0; 10^{-11}; 10^{-10}; 10^{-9}; 10^{-8} ; 10^{-7}; 10^{-6}; 10^{-2} M in Tris-HCl buffer; (D) The corresponding calibration curve of current vs. the concentration of thrombin; (E) Selectivity of the Dual-Hairpin DNA structure assay

for thrombin analysis in Tris-HCl buffer (0.01 M thrombin or other equal concentration proteins as example); (F) Selectivity of the Dual-Hairpin DNA structure assay for thrombin analysis in Tris-HCl buffer containing 10^{-9} M thrombin and other equal concentration proteins or only containing other three equal concentration proteins as example.

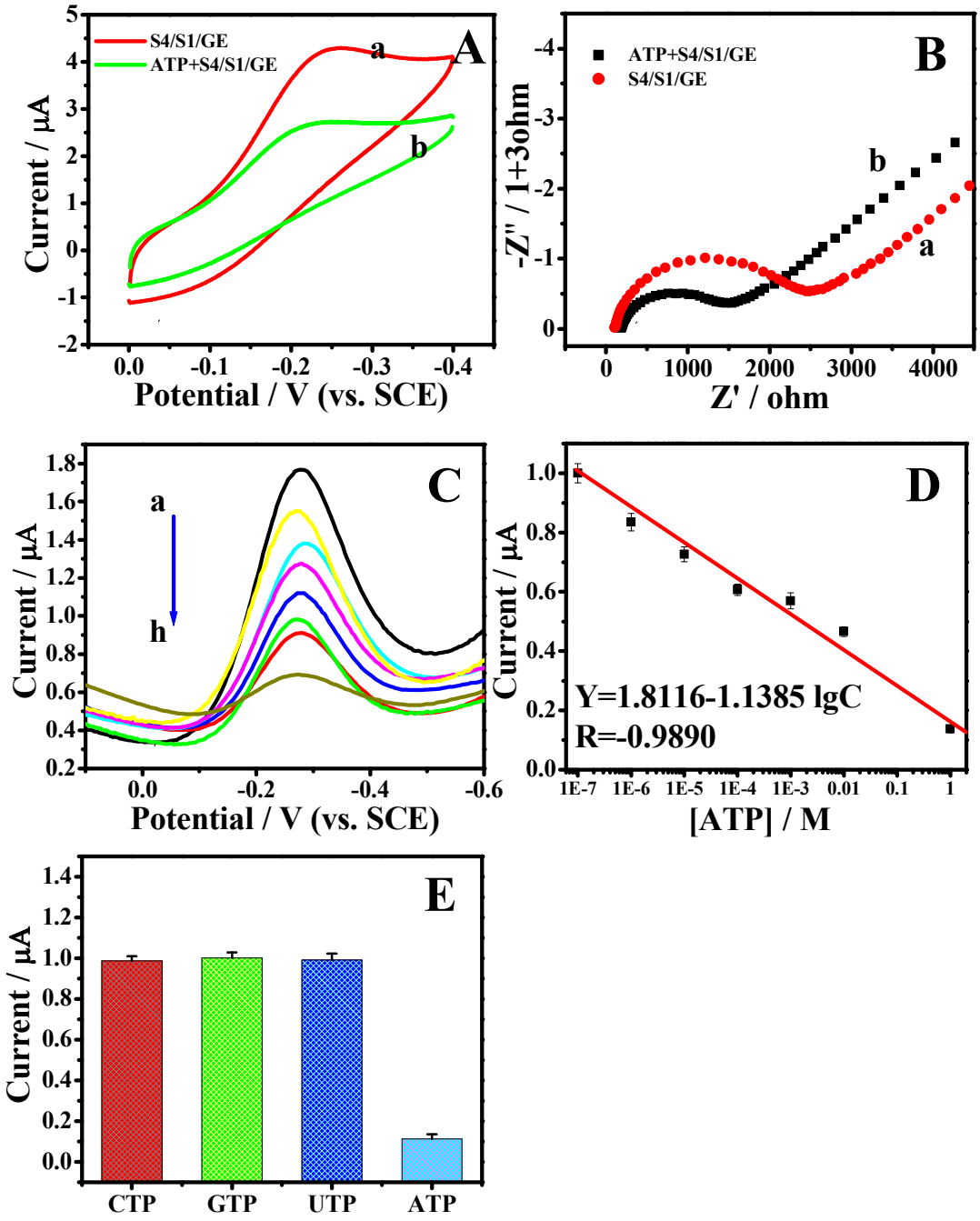

Fig. 5 (A) CV and (B) EIS on Dual-Hairpin DNA structure S4/S1/GE (a); ATP+S4/S1/GE (b), 10^{-4} M ATP as example; (C) DPV and corresponding calibration curve of current vs. the concentration of ATP: (a–h) 0; 10^{-7}; 10^{-6}; 10^{-5}; 10^{-4}; 10^{-3}; 10^{-2}; 1 M in Tris-HCl buffer; and (E) Selectivity of ATP analysis in Tris-HCl buffer (1 M thrombin or other equal concentration substances as example).